Dust Charging in Collisional Plasma in Cryogenic Environment

Natsuko UOTANI, Jumpei KUBOTA, Wataru SEKINE, Megumi CHIKASUE, Masako SHINDO and Osamu ISHIHARA

Faculty of Engineering, Yokohama National University
79-5 Tokiwadai, Hodogaya-ku, Yokohama 240-8501, Japan

(Received: 30 October 2009 / Accepted: 31 January 2010)

Dust charging in a plasma in cryogenic environment is studied experimentally. RF helium plasmas are produced at cryogenic temperature as well as at room-temperature. Dust particles introduced into a plasma are tracked by CCD camera and analyzed by PTV (Particle Tracking Velocimetry) method. Dust charges in a wide range of temperature and pressure are determined by two ways, (1) oscillating trajectory of a dust particle around an equilibrium position in a sheath and (2) deflected trajectory of a charged dust particle coming out of plasma in DC electric field. Dust charge in cryogenic environment is found to be lower than the one at room-temperature. The observed lower charge states are explained by a model with cryogenic ion temperature and ion-neutral collisions.

Keywords: complex (dusty) plasma, strongly coupled system, dust charge, collisional effect, temperature effect, liquid helium, decharging process

1. Introduction

Dust particles in a plasma have been studied extensively over the last few decades. A complex (dusty) plasma is a plasma with micron size dust particles and has been attracting much attention to the community of industrial plasma, space plasma as well as laboratory plasma [1,2]. Recent study of complex plasma has been extended to fusion plasma since dust particles originated from plasma-surface interaction were observed in fusion devices [3,4]. In fusion, industrial or space plasmas dust particles are born in a plasma, but laboratory complex plasma can be produced easily by injecting solid (conductive or dielectric) particles into a plasma. Dust particles immersed in a plasma are charged negatively because of higher mobility of electrons than ions. The charge of a dust particle with a radius of 1~10 μm is typically -10^3e~-10^5e, where e is elementary charge. Because of the nature of large charge of a dust particle, Coulomb coupling parameter Γ defined by a ratio between Coulomb potential energy and kinetic energy of dust particles could be higher than 1 under laboratory plasma conditions. Larger coupling parameters ($\Gamma \gg 1$) characterize the ordered structure of dust particles called Coulomb crystal [5-7]. Recent experiments on complex plasmas are focused on microgravity condition to investigate the nature of a complex system in a three-dimensional symmetrical plasma [8,9].

A cryogenic complex plasma is an emerging field to study dust-plasma interaction in an extreme condition [10,11]. Earlier experimental studies suggested the possible production of cryogenic plasma by pulse discharge in liquid helium [12,13] and ultracold plasma by a method of laser cooling [14]. A DC discharge plasma with dust particles in cryogenic condition was produced and interparticle distance between dust particles was reported to decrease with decreasing temperature [15-17], while our experiment showed constant interparticle distance in a background temperature of 77K and 300K [18]. Figure 1 shows our recent experimental results in the range of 4.2K to 300K. Theoretical study on cryogenic complex plasma suggested two-dimensional dust structure on the surface of liquid helium [19] and a quantum effect on a pair of dust particles [11]. The Coupling parameter Γ could be much higher than 1 on the surface of liquid helium, so the two-dimensional system of charged dust particles is expected to be observed in the crystal phase.

Dust charge is a fundamental parameter for a complex plasma and is needed to be explored in detail under a cryogenic condition. Interactions of dust particle with electrons, ions and dust particles are determined by their charge states. We determined dust charge experimentally by using two experimental setups. Dust

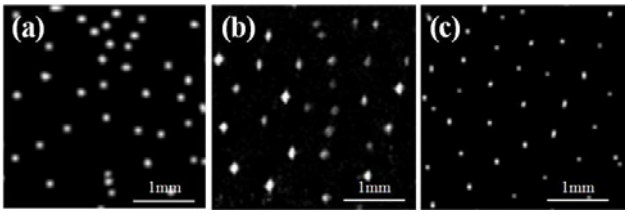

Fig. 1. Observed Coulomb cluster of dust particles in horizontal plane for [T_n(K), P(Pa)] = (a) [4.2, 0.9] (b) [77, 60] (c) [300, 60]. Interparticle distance is d~0.5mm.

author's e-mail: d09gd208@ynu.ac.jp (N. U.)

particles are introduced to a helium plasma produced in cryogenic gas [18,20] or in liquid helium vapor [21].

In this paper, we present background temperature and collisional effects on dust charges. In Sec. 2, experimental observation of dust oscillations under cryogenic condition and a model for charge determination are described. In Sec. 3, we show deflected trajectories of dust particles in the vapor of liquid helium between parallel electrodes and decharging process of dust particles. In Sec. 4, determined dust charge state is discussed. The paper is concluded with results and discussion in Sec. 5.

2. Helium plasma in cryogenic gas (YD-1)

A. Experimental setup

Our experimental setup was described briefly in Ref. [18]. In our earlier experiment, dynamics of dust particles in RF helium plasma was studied in vertical long glass tube at room-temperature [22] as well as at cryogenic temperature [18,20]. The cryogenic experimental apparatus YD-1 (Yokohama Dewar No. 1) is a double silver-coated glass Dewar bottles with the inner diameter of 9.6 cm and the height of 80 cm. Two Dewer bottles have about 1 cm wide vertical uncoated slit on their sides for observation of a complex plasma. The inner Dewar bottle filled with liquid helium (LHe) or liquid nitrogen (LN_2) is placed in outer Dewar bottle. Outer Dewar bottle filled with liquid nitrogen helps keeping cryogenic liquid longer by avoiding inflow of heat. A discharge glass tube set in inner Dewar bottle is shown in Fig. 2. The glass tube is ~70 cm in length consisting of a thin upper part of 60 cm in length with 1.6 cm in inner diameter and a thick lower part of ~12 cm in length with 5 cm in diameter. The glass tube is connected to an external stainless steel pipe at the flange attached to the inner Dewar bottle. An RF helium plasma with a neutral gas pressure $P = 0.1$~100 Pa is produced in the lower part of the glass tube by applying RF (13.56 MHz) voltage of ~50 V between two ring plate electrodes of 4 cm in outer radius and 1 cm in inner radius. Neutral pressure is measured by capacitance diaphragm gauge placed above the flange. The plasma is characterized by the electron density of $n_e \sim 10^{15}$ m^{-3} and electron temperature T_e of a few eV, while ions lose their kinetic energy through collisions with cooled neutrals. The background gas temperature is controlled by containing the cryogenic liquid, liquid helium or liquid nitrogen, in the inner Dewar bottle. Acrylic particles (dust particles) of $a = 0.4$~10 μm in radius with a mass density of $\rho_d = 1.2$ g/cm^3 are dropped from dust dropper situated about 80 cm high from the bottom of the glass tube. The dust particles charged in the plasma are suspended around an equilibrium position where the sheath electric force balances with the downward gravitational force. The equilibrium height from the bottom of the glass tube $h_{eq} =$ 5~30 mm depends on the temperature and pressure conditions. The dust particles illuminated by green laser ($\lambda = 532$ nm) are visible by naked eyes.

To observe vertical motion of a dust particle in the plasma, particles are dropped from the dust dropper. Dust particles are accelerated in the long glass tube under the gravity. The dust particles immediately charged after entering the plasma go further below the equilibrium position and go deeper in the sheath. The electric force acts upward on a negatively charged dust particle in the sheath moves the particle upward against gravity. Dust motion is recorded by high-speed CCD camera from the side at a frame rate of 100~400fps, and analyzed by using PTV (Particle Tracking Velocimetry) method. In PTV method velocity and acceleration are measured by detection of the particle position in each frame. Our earlier experiment showed two dust particles to form vertical pair moving upward along the ion flow in the sheath affected by the wake field [22].

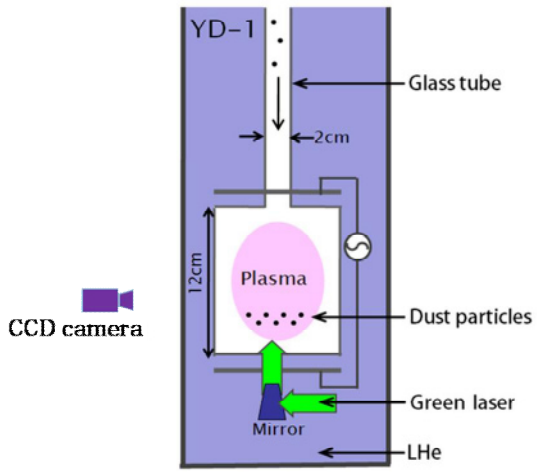

Fig. 2. Experimental setup of YD-1. RF helium plasma is produced in a glass tube surrounded by cryogenic liquid.

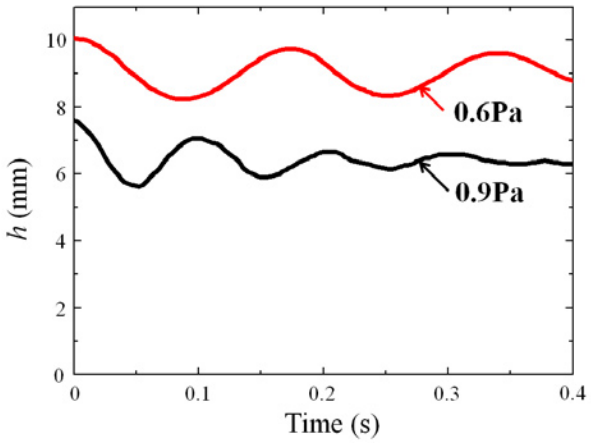

Fig. 3. Damped dust oscillations around equilibrium positions at 4.2K for (1) 0.6 Pa and (2) 0.9 Pa. The equilibrium position, the oscillation frequency and decay time constant depend on the neutral pressure.

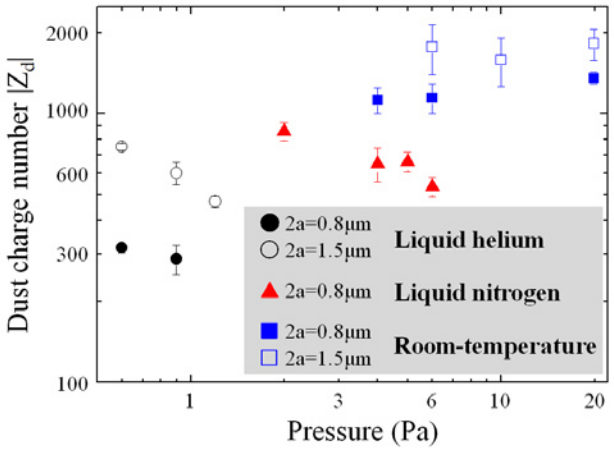

Fig. 4. Dust charge with diameter $2a = 0.8, 1.5$ μm as a function of pressure for 300 K, 77 K and 4.2 K. Dust charges change with temperature while dust charges remain nearly constant with the variation of pressure.

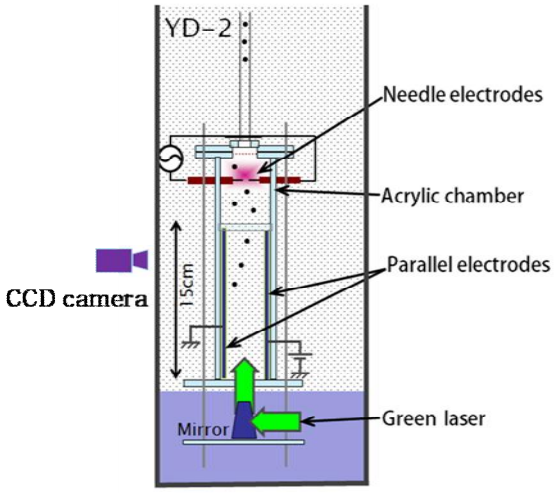

Fig. 5. Experimental setup of YD-2. Plasma is produced in the liquid helium vapor.

B. Neutral temperature in helium plasma

Temperature of neutral particles in RF helium plasma is determined by observing vertical dust oscillation in a liquid nitrogen condition [18]. Figure 3 shows typical damped oscillations around equilibrium positions of $2a = 0.8$ μm in a cryogenic (LHe) condition for various pressures. Dust trajectory under cryogenic temperature as well as room temperature is described by the equation of motion for a damped harmonic oscillator, $m_d\ddot{h}+\gamma\dot{h}+k(h-h_{eq})=0$, where m_d is mass of a dust particle, h is vertical height of a dust particle, γ is friction coefficient of neutral gas and k is a spring constant in the dust oscillation motion. Frequency of dust oscillation ω, equilibrium height h_{eq} and damping time constant τ_d is measured from the trajectories. The friction coefficient γ determined by $2m_d/\tau_d$ is typically $\sim 10^{-15}$ kg/s for neutral density $n_n \sim 10^{22}$ m^{-3} and background helium temperature $T_n \sim 4.2$ K, which agrees reasonably well with the friction coefficient given by Epstein [23] as

$$\gamma = \gamma(T_n) = \delta\left(\frac{4\pi}{3}\right) n_n m_n a^2 c_n(T_n), \qquad (1)$$

where δ is a constant value with 1.0~1.44 depending on the type of reflection, m_n is mass of a neutral particle and $c_n=(\pi k_B T_n/8m_n)^{1/2}$ is mean velocity of neutrals (k_B : the Boltzmann constant). The background helium gas temperature in the glass tube is sufficiently cooled by surrounding cryogenic liquid while producing RF helium plasma [18].

C. Dust charge in cryogenic helium plasma

Experiment at cryogenic temperature is carried out. Various sizes of dust particles with $2a = 0.8$, 1.5, 3, 5, 10, 20 μm are dropped from the dust dropper and are fully charged in the plasma. Smaller dust particles are suspended in the sheath electric field, while lager dust particles reach the bottom of the glass tube without suspension. The dust suspension is observed for $2a \leq 10$μm at 300K, $2a \leq 5$μm at 77K and $2a \leq 3$μm at 4.2K.

Dust charge number $|Z_d|$ is determined by [18,24,25]

$$|Z_d| = \sqrt{2\pi\varepsilon_0 a m_d h_0^2(\omega^2+\tau_d^{-2})/e^2}, \qquad (2)$$

where ε_0 is permittivity of vacuum and $h_0=h_{eq}-m_d g/k$ (g: gravitational acceleration). Typical values of ω = 30~150 rad/s, $\tau_d^{-1} = 2\sim15$ sec^{-1} and $h_{eq} = 5\sim30$ mm depend on temperature and pressure. Dust frequency ω and inversed decay time constant τ_d^{-1} are found to increase with pressure, while equilibrium height h_{eq} is lowered. Figure 4 shows dust charge with $2a = 0.8$ and 1.5 μm. The charge is found to decrease with decreasing background temperature T_n. Dust charges with $2a = 0.8$ μm are smaller than the values of dust charges with $2a$=1.5 μm in the temperature range of 4.2K to 300K.

3. Plasma above liquid helium surface (YD-2)

A. Experimental setup

The cryogenic apparatus YD-2 (16 cm in inner diameter and 1 m in height) is used to produce a plasma in a liquid helium vapor as shown in Fig. 5. A localized plasma in the liquid helium vapor is produced by applying RF voltage between needle electrodes. The RF discharge plasma is produced by applying voltage (10kHz, ~6kV) to tungsten wire needle electrodes. The two needles are separated by 1~2 mm and mounted on an acrylic plate having the central hole 18 mm in diameter. The liquid helium is kept in a superfluid state by decreasing the pressure below 0.1 atm. The plasma with neutral density of $n_n \sim 10^{26}$ m^{-3} is produced locally near the electrodes in high gas pressure (6~8kPa) with the electron density $n_e \sim 10^{15}$ m^{-3} and electron temperature T_e ~ 5 eV, characterizing the electron Debye length $\lambda_{De} \sim 0.5$

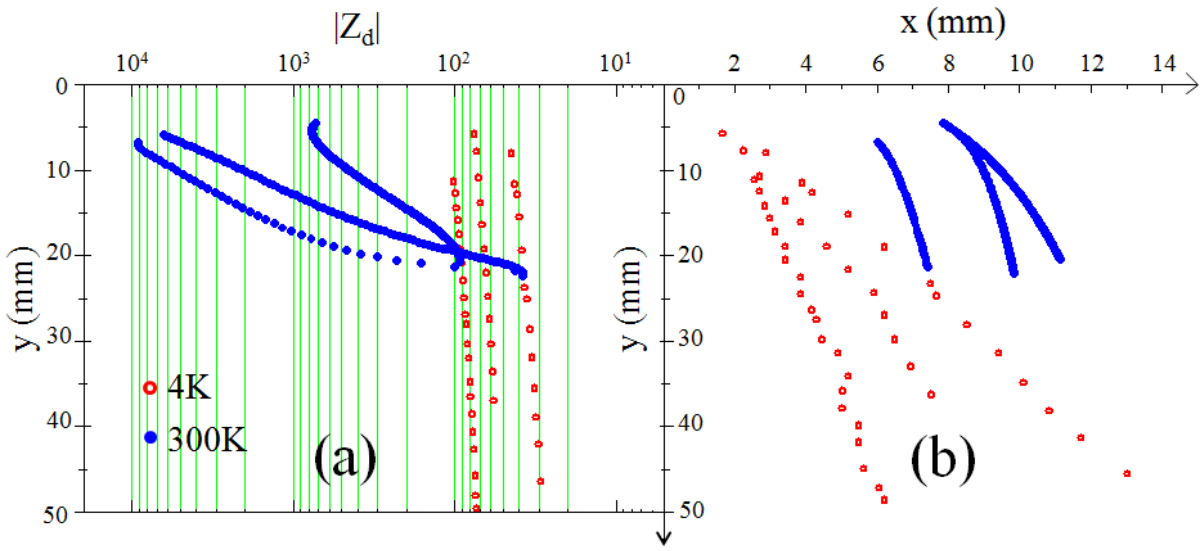

Fig. 6. (a) Charge variation in y direction. (b) Deflected dust trajectory in (x, y) plane. Distance y is measured from the lower edge of the localized plasma. Dust charge decreases with distance away from the plasma. Time interval between recorded points is 2.5 msec and dust particles are shown to move faster at 4 K than 300 K.

mm. Dust particles are supplied from a dust dropper near the flange and fall through thin stainless steel tube of 1 m in length with 2 mm in diameter. Once dust particles reach the needles, they are charged by the plasma. Dust particles gain enough energy by gravitational field before reaching the plasma to move through the plasma and go downward further away from the plasma. Then charged dust particles enter the region where two parallel plates produce electric field in the horizontal direction. Dust particles are deflected in the electric field and their trajectories are recorded by CCD camera. Since the plasma extends hardly to the region between the parallel electrodes, as confirmed by a probe, electric field between two parallel electrodes is approximated by the vacuum field.

B. Model of charge determination

The trajectories of the dust particles with dust charge $Q=Z_d e$ and mass m_d in the electric field $\mathbf{E}$ are described by

$$\frac{Q}{m_d}=\frac{\mathbf{E}\cdot(\ddot{\mathbf{x}}+\gamma\dot{\mathbf{x}})}{E^2}, \tag{3}$$

where $\dot{\mathbf{x}}$ and $\ddot{\mathbf{x}}$ are velocity and acceleration of a dust particle at location $\mathbf{x}$, respectively. And $\mathbf{x}=(x,y)$, x is in the horizontal direction and y is in the gravitational direction with the origin at the center of the needle electrodes. The friction on a dust particle is caused by collisions between dust particles and neutral helium atoms. The friction coefficient γ is given by

$$\gamma=\left(1-\frac{\mathbf{g}\cdot\ddot{\mathbf{x}}}{g^2}\right)\frac{g^2}{\mathbf{g}\cdot\dot{\mathbf{x}}}. \tag{4}$$

By setting $\mathbf{E}=E\mathbf{e}_x$ and $\boldsymbol{g}=g\mathbf{e}_y$. Eq. (3) can be expressed in terms of velocity components as

$$\frac{Q}{m_d}=\frac{1}{E}[\dot{v}_x-(\dot{v}_y-g)\tan\theta], \tag{5}$$

where $\tan\theta=v_x/v_y$. The values of θ, $\dot{v}_x$ and $\dot{v}_y$ are measured by PTV method. The variable DC voltage in the range of ±300 V is applied between the two parallel plates (8 cm by 3.4 cm) separated by 4.2 cm. The electric field under the plasma is produced uniformly in the x direction. Any effect by the diffused plasma to the electric field is negligible because of the localized nature of the plasma. Charged dust particles are observed to fall without deflection in the absence of electric field.

C. Deflected trajectory between DC electrodes

The bright discharge plasma extends to a region of about ~1 mm in thickness and ~1 cm in width. The falling dust particles pass through the hole on the acrylic plate with the thickness of 5 mm. The period to cross the plasma region is about 0.01 sec, which is sufficiently longer than charging time ~10^{-7} sec. Observed positions of typical dust particles and their charges at the point are shown in Fig. 6. Deflected direction of trajectories confirms the charging state of dust particles as negative. Charges of dust particles are found to decrease exponentially as dust particles leave the plasma. To confirm the cryogenic effect on the decharging process, we produced helium plasma at 300 K, 1~10 kPa with the same background neutral density in the liquid helium vapor and measured charges of dust particles. Charges of a dust particle are found to be several times larger than the one in cryogenic environment. The friction

coefficients are estimated as $\gamma \sim 10^{-12}$ kg/s at 300 K and $\gamma \sim 10^{-13}$ kg/s at 4 K. The viscosity of helium gas decreases as temperature reduction. We found $Q \sim$ -500e for $a = 1.5$ μm, $\rho_d = 1.2$ g/cm^3.

Since many electrons are attached to dust surface a massive dust particle behaves as a negative charge career in a plasma. Charge to mass ratio of a particle characterizes its dynamics in a complex plasma. Charge to mass ratio of a dust particle $|Q|/m_d \sim 5\times10^{-3}$ C/kg is much smaller than electron charge to mass ratio $e/m_e = 1.76\times10^{11}$ C/kg. But the charge of dust particle is enough to respond to electric force.

It should be noted that some dust particles are observed to be trapped in the plasma or deflected by the plasma in spite of injecting velocity ~15 cm/s at the upper plasma boundary. Dust particles fall through a thin stainless tube of 1 m in length with 2 mm in diameter. Dust particles collide with the tube while they fall and the velocities of dust particles at the exit of the tube are not uniform. Dust particles having velocity less than 15 cm/s are trapped easily in the plasma. There may be neutral flow over the plasma by thermophortic force.

4. Discussion

A. Decharging process in the liquid helium vapor

Decharging process in a vapor above the superfluid liquid helium as well as in a helium gas at room-temperature is discussed in this section. Experiments on decharging process were conducted in discharge afterglow under microgravity condition [26] as well as an on-ground condition by using thermophoretic force [27]. Electric field with a frequency of a few Hz was applied to the dust particle floating in the afterglow plasmas, and a rest charge on a dust particle was estimated based on the dynamics of dust motion. It should be noted that dust particles stay in afterglow plasma in these experiments, while dust particles pass through the localized plasma and move out of the plasma in our experiment.

Deflected dust trajectory and spatial variation of dust charge are shown in Fig. 6. As can be seen in Fig. 6, dust charge decreases exponentially with time as $|Z_d(y)| = |Z_d|\exp(-y/l_y)$, where l_y is decharging length and l_y = 10~100 mm at 4 K and $l_y \sim 4$ mm at 300 K.

The charging frequency ω_c in a collisionless plasma is given by $\omega_c \sim (a/\lambda_{Di})\omega_{pi}$ [1], while $\omega_c \sim (l_i/\lambda_{Di})\omega_{pi}$ in collsional plasma [28], where $\omega_{pi} = (n_i e^2/\varepsilon_0 m_i)^{1/2}$ is ion plasma frequency, n_i is ion density and m_i is a ion mass. In the plasma above liquid helium surface, charging frequency is $\omega_c \sim 10^6$ rad/s. Since dust particles have velocity on the order of $v_y \sim 10$cm/s, $\omega_c/2\pi$ is much higher than the value of $v_y/l_y \sim 10$ sec^{-1}. Time dependence of decharging process of dust charges was studied in an afterglow plasma [26,27], while we have measured space dependence of dust charges above liquid helium surface by observing dust trajectories passing through a localized plasma.

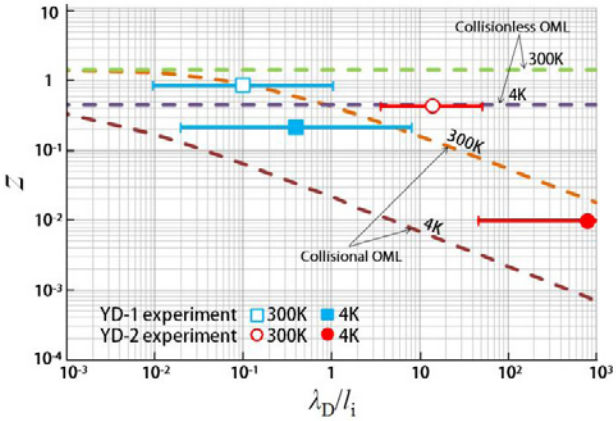

Fig. 7. Normalized dust charge z as a function of collision parameter λ_D/l_i. Experimental values, theoretical values of collisionless OML theory and collisional OML theory are shown.

B. Lower charge state in a cryogenic plasma

The dust charges determined by two different methods suggest that charges decrease with decreasing temperature. Comparing the results of YD-1 and YD-2 at the same temperature condition, charge obtained by YD-2 is smaller than YD-1. Lower charge state of dust particles is discussed in this section.

It was shown by simulation that charge exchange of ion on neutrals affects the charge state at room-temperature [29] as well as cryogenic temperature [17]. A cross section of charge exchange collision σ is $\sigma \sim 5\times10^{-19}$ m^2. Ion mean free path l_i in YD-1 is estimated as $l_i \sim 1$ mm at 300 K, $l_i \sim 1$mm at 77 K and $l_i \sim 0.1$ mm at 4.2 K. In YD-2 with higher neutral pressure the ion mean free path is $l_i \sim 0.1$ μm at 4 K, $l_i \sim 0.01$ mm at 300 K. Ions in the plasma are assumed to be cooled by neutral-ion collisions ($T_i \sim T_n$) since dimensions of plasma L ($L \sim 50$ mm in YD-1 experiment, $L \sim 10$ mm in YD-2 experiment) are much larger than the ion mean free path ($L \gg l_i$). Because of the energy supplied to maintain the plasma and the longer nature of mean free path of electrons than ions, electrons keep their thermal energy. For our experiments, electron Debye length λ_{De} of our plasma is $\lambda_{De} \sim 0.5$ mm, while ion Debye length λ_{Di} changes its value λ_{Di} = 4~40 μm at 4~300 K.

The effect of ion-neutral collisions on charging was shown in series of experiments [30,31]. Ion current in the presence collisions is given by [31]

$$I_i = \sqrt{8\pi}\, a^2 n_i v_{Ti} z\tau[1 + 0.1z\tau(\lambda/l_i)], \qquad (6)$$

where $v_{Ti} = (2k_B T_i/m_i)^{1/2}$ is thermal velocity of ions, τ is temperature ratio $\tau = T_e/T_i$, z is normalized dust charge

$$z = \frac{|z_d| e^2}{4\pi\varepsilon_0 a k_B T_e}, \quad (7)$$

To calculate the dust charge it is necessary to equate the ion flux to the electron flux $I_e=\sqrt{8\pi}a^2 n_e v_{Te}\exp(-z)$, where where $v_{Te}=(2k_BT_e/m_e)^{1/2}$. The dust charges by collisionless OML theory and collisional OML theory are compared to our experimental data. Figure. 7 shows normalized dust charge z as a function of normalized collision parameter λ_D/l_i. The ambiguity of our experimental data in normalized collision parameters is derived with λ_{De} or λ_{Di}. The lower charge state in cryogenic condition and in collisional situation is clearly shown to agree with theoretical predictions as shown in Fig 7.

5. Conclusions

RF helium plasmas are produced in cryogenic gas as well as in liquid helium vapor. Dust particles introduced into the plasmas are tracked by CCD camera and analyzed by PTV method. Dust charges in a wide range of temperature and pressure are determined by two ways, oscillating trajectory of dust particles around equilibrium position and deflected trajectory of charged dust particles in DC electric field. The dust charge in cryogenic environment is found to be much lower than the one at room-temperature. Background cryogenic temperature and collisions lead lower charge state at cryogenic condition.

Acknowledgments

This work is supported by Asian Office of Aerospace Research and Development under award number AOARD-08-4116 and JSPS (Japan Society for the Promotion of Science) Grant-in-Aid for Scientific Research (B) under Grant No.19340173.

References

[1] O. Ishihara, J. Physics D: Appl. Phys. **40**, R121 (2007).
[2] G. E. Morfill and A. V. Ivlev, Rev. Mod. Phys. **81**, 1353 (2009).
[3] J. Winter, Plasma Phys. Controlled Fusion **40**, 1201 (1998).
[4] N. Ohno, M. Yoshimi, M. Tokitani, S. Takamura, K. Tokunaga and N. Yoshida, J. Nucl. Mater. **390**, 61 (2009).
[5] J. H. Chu and Lin I, Phys. Rev. Lett. **72**, 4009 (1994).
[6] H. Thomas, G. E. Morfill, V. Demmel, J. Goree, B. Feuerbacher and D. Mohlmann, Phys. Rev. Lett. **73**, 652 (1994).
[7] Y. Hayashi and K. Tachibana, Jpn. J. Appl. Phys. **33**, 804 (1994).
[8] A.V. Ivlev, G. E. Morfill, H. M. Thomas, C. Räth, G. Joyce, P. Huber, R. Kompaneets, V. E. Fortov, A. M. Lipaev, V. I. Molotkov, T. Reiter, M. Turin, and P. Vinogradov. Phys. Rev. Lett. **100**, 095003 (2008).
[9] K. R. Sütterlin, A. Wysocki, A.V. Ivlev, C. Räth, H. M. Thomas, M. Rubin-Zuzic, W. J. Goedheer, V. E. Fortov, A. M. Lipaev, V. I. Molotkov, O. F. Petrov, G. E. Morfill, and H. Löwen, Phys. Rev. Lett. **102**, 085003 (2009).
[10] O. Ishihara, in *Multifacets of Dusty Plasmas*, edited by J.T. Mendonça, D. P. Resends and P. K. Shukla, AIP Conference Series, vol. 1041 (Melville, N.Y., AIP, 2008) pp. 139.
[11] O. Ishihara, W. Sekine, J. Kubota, N. Uotani, M. Chikasue, and M. Shindo, in *New Developments in Nonlinear Plasma Physics*, ed. by B. Eliasson and P. K. Shukla (Melville, N.Y., AIP, 2009) p. 110.
[12] K. Minami, Y. Yamanishi, C. Kojima, M. Shindo, and O. Ishihara, IEEE Trans. on Plasma Sci. **31**, 429 (2003).
[13] C. Kojima, K. Minami, W. Qin, and O. Ishihara, IEEE Trans. on Plasma Sci. **31**, 1379 (2003).
[14] T. C. Killian, S. Kulin, S. D. Bergeson, L. A. Orozco, C. Orzel, and S. L. Rolston, Phys. Rev. Lett. **83**, 4776 (1999).
[15] V. E. Fortov, L. M. Vasilyak. S. P. Vetchinin, V. S. Zimmukhov, A. P. Nefedov and D. N. Polyakov, Doki. Phys. **47**, 21 (2002).
[16] S. N. Antipov, E. I. Asinovskii, V. E. Fortov, A. V. Kirillin, V. V. Markovets, O. F. Petrov and V. I. Platonov, Phys. Plasmas **14**, 090701 (2007).
[17] S. N. Antipov, E. I. Asinovskii, A. V. Kirillin, S. A. Maiorov, V. V. Markovits, O. F. Petrov and V. E. Fortov, JETP. **133**, 830 (2008).
[18] J. Kubota, C. Kojima, W. Sekine and O. Ishihara, J. Plasma Fusion Res. Series **8**, 286 (2009).
[19] M. Rosenberg and G. J. Kalman, Europhys. Lett. **75**, 894 (2006).
[20] J. Kubota, C. Kojima, W. Sekine and O. Ishihara, in *Multifacets of Dusty Plasmas*, edited by J.T. Mendonça, D. P. Resends and P. K. Shukla, AIP Conference Series, vol. 1041 (Melville, N.Y., AI P, 2008) p. 235.
[21] M. Shindo, N. Uotani and O. Ishihara, J. Plasma Fusion Res. Series **8**, 294 (2009).
[22] C. Kojima, J. Kubota, Y. Tashima, and O. Ishihara, J. Jpn. Soc. Microgravity Appl. **25**, 353 (2008).
[23] P. S. Epstein, Phys. Rev. **23,** 710 (1924).
[24] E. B. Tomme B. M. Annaratone, and J. E. Allen, Plasma Sources Sci. Technol. **9**, 87 (2000).
[25] E. B. Tomme, D. A. Law, B. M. Annaratone and J. E. Allen, Phys Rev. Lett. **85**, 2518 (2000).
[26] A.V. Ivlev, M. Kretschmer, M. Zuzic, G. E. Morfill, H. Rothermel, H.M. Thomas, V. E. Fortov, V. I. Molotkov, A. P. Nefedov, A.M. Lipaev, O. F. Petrov, Yu.M. Baturin, A. I. Ivanov, and J. Goree, Phys. Rev. Lett. **93**, 055003 (2004).
[27] L. Couëdel, M. Mikikian, L. Boufendi, A. A. Samarian, Phys. Rev. E **74**, 026403 (2006).
[28] S. A. Khrapak, G. E. Morfill, A. G. Khrapak and L. G. D'yachkov, Phys. Plasmas **13**, 052114 (2006).
[29] A. V. Zobnin, A. P. Nefedov, V. A. Sinel'shchikov and V. E. Fortov, JETP. **91**, 483 (2000).
[30] S. Ratynskaia, S. Khrapak, A. Zobnin, M. H. Thoma, M. Kretschmer, A. Usachev, V. Yaroshenko, R. A. Quinn, G. E. Morfill, O. Petrov and V. Fortov, Phys. Rev. Lett. **93**, 085001 (2004).
[31] S. A. Khrapak, S. V. Ratynskaia, , A. V. Zobnin, A. D. Usachev, V. V. Yaroshenko, M. H. Thoma, M. Kretschmer, H. Höfner, G. E. Morfill, O. F. Petrov and V. E. Fortov, Phys. Rev. E **72**, 016406 (2005).